

# Preparation, characterization and magnetic properties of an ordered FeCo single crystal

S.-Y. Chu, C. Kline, M.-Q. Huang, and M. E. McHenry<sup>a)</sup>

*Department of Materials Science and Engineering, Carnegie Mellon University, Pittsburgh, Pennsylvania 15213*

J. Cross and V. G. Harris

*U. S. Naval Research Laboratory, Washington, DC 20375*

Pristine FeCo single crystals with millimeter dimensions were prepared by annealing FeCo ingot samples. The composition and microstructure of a fine polished cylindrical single crystal specimen used in this work were characterized by energy dispersive x-ray analysis, scanning electron microscopy, back-reflection Laue diffraction photographs, and x-ray diffraction (XRD). The ordered  $\alpha'$  phase in the specimen was detected by XRD experiments using the synchrotron light source at Brookhaven National Laboratory. The full width at half maximum of the superlattice line, i.e., the (100) reflection, in phi scan was  $2.5^\circ$ . The magnetic field dependence of the magnetic moment was measured with the field oriented in different directions using a superconducting quantum interference device magnetometer and a vibrating sample magnetometer. © 1999 American Institute of Physics. [S0021-8979(99)17308-0]

## I. INTRODUCTION

Magnetic property measurements of Fe–Co alloys date back more than half a century.<sup>1–3</sup> These alloys have significant advantages for soft magnetic material applications that include a very high saturation magnetization, a high Curie temperature, and low magnetocrystalline anisotropy. Recently, great interest in the reinvestigation of these alloys has been raised for their application in airborne electrical devices operating at high temperatures.<sup>4–6</sup> For example, Hiperco50 is a Carpenter Steel high induction soft magnetic Fe–Co alloy which is currently used as a rotor material in aircraft engines.

Fe–Co alloys exhibit the largest magnetic induction of any material (i.e., are at the peak of the Slater–Pauling curve). Alloys near the equi-atomic composition are particularly soft and exhibit large permeabilities.<sup>7</sup> This magnetic softness is rooted in a zero crossing of the first-order magnetic anisotropy constant,  $K_1$ , near this composition.  $V$  additions are made for metallurgical reasons and to increase alloy resistivity and therefore decrease eddy current losses in these soft materials. These additions reduce the magnetic moment. Fe–Co alloys undergo an order–disorder transformation at a maximum temperature of  $725^\circ\text{C}$  at the composition  $\text{Fe}_{50}\text{Co}_{50}$ , with a change in structure from the disordered BCC(A1) to the ordered CsCl(B2)-type structure.

In order to have accurate measurements of physical constants and heat treatment effects in these materials, high quality single crystals are necessary. Most of the published data in the literature on FeCo alloys are based on experiments performed in the 1930's.<sup>8</sup> Crystal quality and experimental techniques available at this time may lead to experimental uncertainty in measurements of such important properties as the magnetocrystalline anisotropy constant.

This has motivated us to prepare and to characterize high quality single crystals of equi-atomic FeCo alloys in the ordered  $\alpha'$  phase.

## II. EXPERIMENTAL PROCEDURE

In order to make a large enough single crystal for subsequent experiments, several pieces of slabs (1.5 mm in thickness) were cut from an ingot sample (Heat P4092, Carpenter Technology Corporation). These were subsequently placed in a vacuum quartz tube and annealed in a resistance furnace for 20 h at  $930^\circ\text{C}$  and quenched at  $710^\circ\text{C}$  after a slow cool with a cooling rate of  $1^\circ\text{C}/\text{min}$ . A few large crystalline grains could be observed in the heat-treated ingot samples after etching with nitric acid.

The crystal used in present work was cut from such a recrystallized ingot. After determining its crystallographic orientation by using a homemade back-reflection Laue x-ray camera, the crystal was finely polished in a cylindrical specimen with a (110) plane observed on both sides. To obtain the ordered FeCo microstructure, the specimen was annealed again in vacuum at  $710^\circ\text{C}$  for 4 h and slowly cooled to room temperature at a cooling rate of  $1^\circ\text{C}/\text{min}$ .

## III. RESULTS AND DISCUSSION

### A. Structure and compositional characterization

Figure 1 illustrates an optical photomicrograph of the cylindrical specimen. Using crystal mass,  $m = 1.434$  mg, and microscopically determined crystal dimensions, 0.810 mm in diameter and 0.342 mm in thickness, we determined the crystal's density to be  $\rho = 8.14$  g/cm<sup>3</sup>. This value is in close agreement with the 8.18 g/cm<sup>3</sup> density determined by the x-ray diffraction (XRD) determined  $\alpha'$  phase lattice parameter. Back-reflection Laue photographs for both sides of the specimen are shown in Fig. 2, where the x-ray beam perpen-

<sup>a)</sup>Electronic mail: mm7g@andrew.cmu.edu

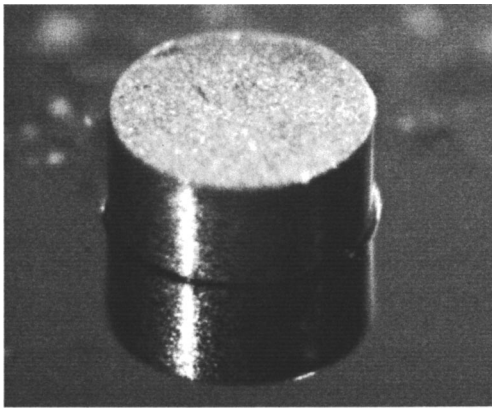


FIG. 1. Optical photomicrograph of FeCo single crystal in the ordered  $\alpha'$  phase.

dicular to each side was mostly in the  $[110]$  crystallographic direction. The perfect symmetry of the patterns and sharpness of the Laue spots are evidence of the high quality of our single crystal specimen. An x-ray diffraction omega scan of the specimen detected that the shift of the  $(110)$  plane from the selected cutting side is less than  $0.6^\circ$  (see Fig. 3).

An energy dispersive x-ray (EDX) pattern of the FeCo specimen was performed in a scanning electron microscope (SEM). It has been confirmed that there were no excess impurity elements introduced in the specimen during the preparation process comparing with a chemical analysis for the raw ingot sample before the heat treatment.

To investigate the microstructure of the  $\alpha'$  phase FeCo, conventional powder diffractometers with sealed filament x-ray tube (Cu  $K\alpha$  radiation) and synchrotron light source [National Synchrotron Light Source (NSLS), Brookhaven National Laboratory] were employed, respectively. A partial x-ray diffraction pattern of the specimen in the range of  $2\theta$  covered from  $10^\circ$  to  $80^\circ$  is illustrated in Fig. 4(a). The only diffraction peaks that can be distinguished are from the  $(110)$  and  $(220)$  planes, respectively. In comparison with a wide peak from a polycrystalline sample, each diffraction peak of the single crystal can be seen as revealing two peaks corresponding to  $K\alpha_1=0.154\ 439$  and  $K\alpha_2=0.154\ 056$  nm wavelengths of the Cu radiation. Based on this experimental data, the lattice parameter of the FeCo single crystal is determined to be  $a=0.285\ 63\pm 0.000\ 02$  nm, which is a very good agreement with a previous literature reported value.<sup>9</sup>

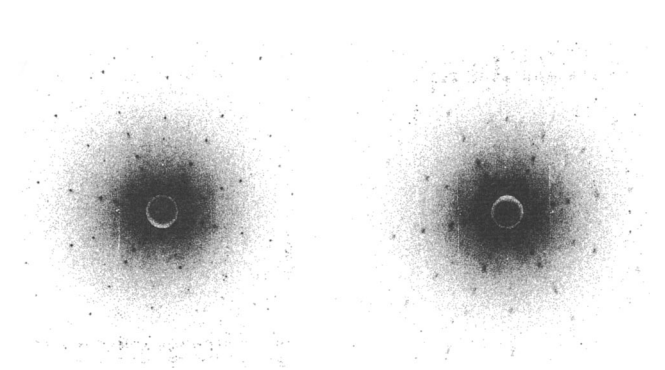


FIG. 2. Back-reflection Laue x-ray photograph of both sides of the cylindrical specimen.

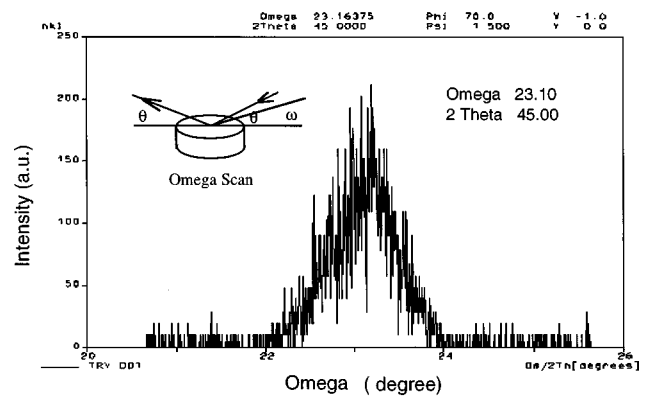


FIG. 3. X-ray diffraction pattern in omega scan on one side of the cylindrical specimen.

To confirm that the separation of each diffraction peak was caused by the different wavelengths, a more accurate measurement was also performed by using a monochromatic beam from synchrotron light source as shown in Fig. 4(b). No double peak can be observed here.

The full width at half maximum (FWHM) of the  $(110)$  reflection in Fig. 4(b), as determined by the synchrotron XRD, is only  $0.05^\circ$ . This implies also that the line broadening of the peak in Fig. 4(a) was mostly instrumental resulting from the “imperfectly parallel beam” provided by the sealed-off filament x-ray tube instead of the “mosaic structure” of our specimen. We believe that some peaks with

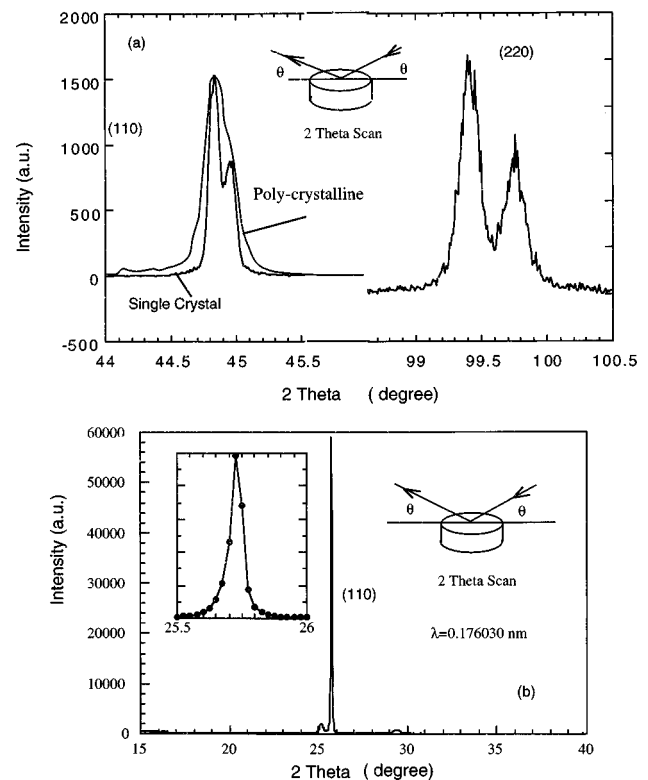


FIG. 4. X-ray diffraction pattern in  $\theta$ - $2\theta$  scanning on one side of the cylindrical specimen. Cu  $K\alpha_1$  and  $K\alpha_2$  radiation (a) and synchrotron light source (b) were used as the x-ray source.

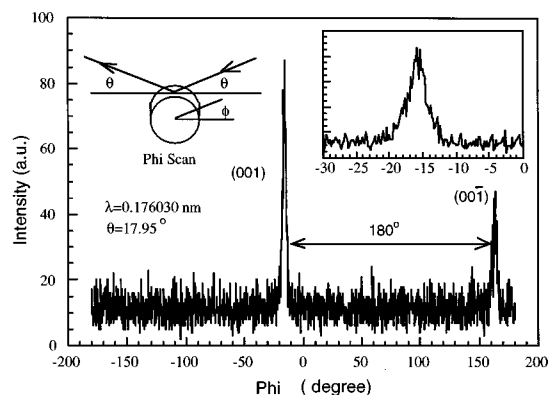


FIG. 5. Observation of the superlattice line, (001) and (00 $\bar{1}$ ) peaks, in phi scan confirms the specimen to be in the ordered  $\alpha'$  phase.

weak intensity in Fig. 4(b) arise from the glass holder, and are not observed in Fig. 4(a) where an oriented silicon (100) holder was used.

It should be noted that the (001) superlattice reflection for FeCo in an ordered  $\alpha'$  phase is difficult to detect with a conventional x-ray powder diffractometer with sealed filament x-ray tube. This is because of the very low intensity relative to that of a fundamental line when the two atoms involved in the alloy, Fe and Co, have nearly the same atomic numbers and therefore nearly identical x-ray scattering factors. A more effective technique for detecting this superlattice reflection is to use a strong synchrotron light source with a wavelength near the  $K$  absorption edge of one of the scattering elements so as to take advantage of anomalous scattering. This anomalous scattering increases the difference in scattering factors for Fe and Co. A detailed description of the anomalous scattering is contained in Ref. 10. Briefly, when a monochromatic x-ray beam with such a wavelength is chosen, the superlattice lines for the ordered phase, (001) peak, for instance, should appear more intensely than for conditions which do not favor anomalous scattering.

Figure 5 shows such an experiment geometry for a synchrotron x-ray scattering experiment and its result. When the specimen was rotated with respect to the [110] axis, i.e., the x-ray beam was parallel to both sides of the cylindrical specimen, two peaks corresponding to (001) reflection and (00 $\bar{1}$ ) reflections appear with a separation of 180° in phi scan. A small FWHM of each superlattice line, 2.5°, is consistent, again, with a large single crystal without mosaic structure. A difference in intensity of the two peaks was caused by a slight shift of the specimen from the center of the x-ray beam.

## B. Magnetic properties

Hysteresis loops of the FeCo single crystal (Fig. 6) have been obtained using a vibrating sample magnetometer (VSM) (model 730, Lakeshore) and a superconducting quantum interference device (SQUID) (MPMSR2, Quantum Design) magnetometers. Based on the data when the applied field is parallel to both sides of the cylindrical specimen, one

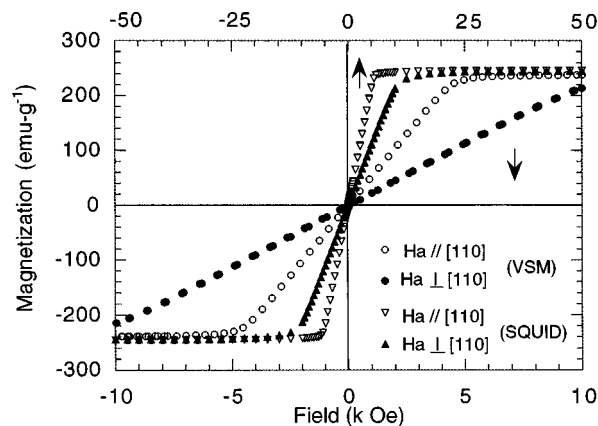


FIG. 6. Hysteresis loops of the FeCo single crystal using a VSM and a SQUID magnetometer, respectively.

has the saturation magnetization,  $I_S$ , to be about 239 emu/g (or 1941 G), which is nearly identical to the data of Couderchon.<sup>8</sup> When the field is applied perpendicular to the faces, the applied field for saturation was rather high (>10 kG) due to large demagnetization effects. For this reason, a SQUID magnetometer with a 5 T superconducting solenoid was employed to measure the dc magnetization of the crystal. With regard to the permeability,  $\mu$ , and magnetocrystalline anisotropy constants,  $K$ , the usual difficulty arises in estimating the demagnetizing factor,  $N$ , making analysis of this data difficult. A detailed analysis on our experimental magnetic anisotropy data will be presented in future work.

## ACKNOWLEDGMENTS

The authors gratefully acknowledge M. S. Masteller of Carpenter Technology Corporation for providing the raw ingot sample. This work was supported by the Air Force Office of Scientific Research, Air Force Material-Command, USAF, under Grant No. F49620-96-1-0454. The U.S. Government is authorized to reproduce and distribute reprints for governmental purposes notwithstanding any copyright notation thereon. Work was carried out in part at the National Synchrotron Light Source, Brookhaven National Laboratory, which is supported by the U.S. DOE, Divisions of Materials Sciences and of Chemical Sciences. Special thanks to Johnny Kirkland for his help on Beamline X23B.

<sup>1</sup>A. Kussmann, B. Scharnow, and A. Schulze-Berlin-Charlottenburg, *Z. Tech. Phys. (Leipzig)* **10**, 449 (1932).

<sup>2</sup>J. W. Shih, *Phys. Rev.* **46**, 139 (1934).

<sup>3</sup>L. W. McKeehan, *Phys. Rev.* **51**, 136 (1936).

<sup>4</sup>D. Gautard, G. Couderchon, and L. Coutu, *J. Magn. Magn. Mater.* **160**, 359 (1996).

<sup>5</sup>J. H. Scott, Z. Turgut, K. Chowdary, M. E. McHenry, and S. A. Majetich, *Mater. Res. Soc. Symp. Proc.* **501** (1998).

<sup>6</sup>Z. Turgut, J. H. Scott, M. Q. Huang, S. A. Majetich, and M. E. McHenry, *J. Appl. Phys.* (in press).

<sup>7</sup>R. Boll, *Materials Science and Technology, A Comprehensive Treatment*, edited by K. H. J. Buschow (1994), Vol. 3B, Chap. 14, p. 399.

<sup>8</sup>G. Couderchon and J. F. Tiers, *J. Magn. Magn. Mater.* **26**, 197 (1982).

<sup>9</sup>T. Nishizawa and K. Ishida, *Bull. Alloy Phase Diagrams* **5**, 250 (1984).

<sup>10</sup>B. D. Cullity, *Elements of X-ray Diffraction*, 2nd ed. (Addison-Wesley, Reading, MA, 1978).